Proc. Estonian Acad. Sci. Phys. Math., 1999, **48**, 3/4, 206–229
https://doi.org/10.3176/phys.math.1999.3/4.05

NONLINEAR EFFECTS IN BICHROMATIC SURFACE WAVES

E. van GROESEN[a], ANDONOWATI[a, b], and E. SOEWONO[b]

[a] Faculty of Mathematical Sciences, University of Twente, P.O. Box 217, 7500 AE Enschede, The Netherlands; groesen@math.utwente.nl
[b] Department of Mathematics, Institut Teknologi Bandung, Jl. Ganesha 10 Bandung, Indonesia

Received 17 March 1999

Abstract. We describe and partly explain the change of the form of bichromatic surface waves with large amplitudes. This phenomenon was recently observed in laboratory experiments and reported by C. T. Stansberg at the Third International Symposium on Ocean Measurement and Analysis (WAVES 97) in 1997. We motivate the use of a Korteweg–de Vries-type equation; improved dispersive properties are necessary in view of the relatively short wavelengths in the experiments. A second-order expansion is shown to be quite capable of describing waves of small and moderate amplitudes. However, waves of extreme amplitude require a more sophisticated attack. Based on phase-amplitude equations of a nonlinear Schrödinger model, we are able to give an analytical description of the phenomenon which provides additional insight into the ingenious pseudo-empirical explanation of Stansberg.

Key words: bichromatic surface wave, nonlinear effect, Korteweg–de Vries-type equation, second-order expansion, phase-amplitude of a nonlinear Schrödinger model, extreme-amplitude wave.

1. INTRODUCTION

The study of various wave phenomena conducted in the past decades has increased our understanding of their theoretical aspects as well as application in different areas. In this paper some typical problems that we have encountered in cooperating with hydrodynamic laboratories are presented. For hydrodynamic laboratories, the generation and control of waves are an essential prerequisite for testing ships in specified wave fields. Below we shall consider some problems of those identified in cooperation between MARIN (Maritime Research Institute, Wageningen, The Netherlands) and IHL (Indonesian Hydrodynamic Laboratory,

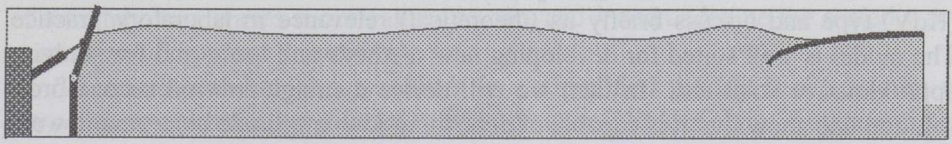

Fig. 1. Schematic cross-sectional view of a typical towing tank with the wave generator on the left and (partially) absorbing "beach" on the right.

Surabaya, Indonesia). The geometry and dimensions of interest are therefore taken as these of the water tanks of the laboratories. In Fig. 1 a schematic cross-sectional view of a typical towing tank is given, which illustrates the division of the tank into three main regions: waves are generated on the left, run "freely" to the right, and are then partly absorbed and partly reflected by the "beach" on the right.

Typical dimensions of such a towing tank are as follows: length 235 m, width 11 m, and undisturbed water depth 5.5 m. In such tanks the performance of ships is tested in operational conditions with waves of various kinds. For an adequate operation of the laboratories understanding of the basic wave patterns is required. With ever increasing demands on testing ships in a specific realistic situation, nowadays the aim is to be able to generate waves that are precisely described at a given position in the basin. For this requirement, the transition should be made from the wave signal at the given position to the corresponding steering of the wave generator, taking into account the position and performance of the wave generator and disturbing effects such as reflection at the beach.

It is clear that for predicting the wave evolution, or determining steering of the wavemaker, accurate quantitative data are required. Even though the basic physical laws describing the water motion are known, it is difficult to generate and simulate the waves because of their inherently nonlinear character, and because of various disturbing effects in the laboratory situation. The full equations for surface waves (restricting to irrotational flows, thus excluding nontrivial currents) can be used in numerical codes. In the cooperation project, an efficient and reliable mixed FEM/FD code, called HUBRIS, has been developed [1]. This 2D code is the basis of a "numerical wave tank" to which an accurate wave generator and partial reflecting beaches are being added with the aim of designing a practical tool for predicting the required generator motion.

To develop such a tool, as well as to be able to interpret the many phenomena observed, it is equally important to study the simplified models theoretically. In this paper we will concentrate on the validity of a particular model and show that even for this simplified model, relevant questions are still difficult to answer in a satisfactory way. One of the major difficulties is that in typical laboratory practice, measurements and information as functions of time are available or requested at a specified position, whereas in theoretical investigations the modern dynamical system theory approach leads more naturally to spatial results at a specified time; we will see various examples of this difference below.

In Section 2 we start with a simple model which will be of Korteweg–de Vries (KdV) type and discuss briefly its (theoretical) relevance in laboratory practice. The model is well suited for developing new methods and tools, and for studying approximative solutions. In fact, we will derive a straightforward second-order solution and show that it is capable of describing low-amplitude bichromatic wave interactions. However, the second-order solution loses its validity in case of longer time or space intervals and larger amplitudes. This will be illustrated on large-amplitude bichromatic waves. The characteristic phenomenon described recently by Stansberg [2], that the envelope of an initially symmetric bichromatic wave steepens and grows in the front and flattens and decreases in the rear, cannot be described with the second-order theory. We will show that an asymptotic model using a nonlinear Schrödinger (NLS)-type equation for the amplitude (and phase) is able to describe the phenomenon. Still, the asymptotic methods described here should be improved further, which calls for a theory and methods that deal with the full nonlinear problem. However, such a theory is not available yet, and to simplify mathematical details, the model equation can be used for the purposes of developing such methods.

2. MODEL EQUATION

In this section we describe a model equation for waves that are relevant in the laboratory situation; boundary effects will be neglected. First, we briefly describe the derivation of the model equation and motivate that the laboratory situation requires that the dispersion be modelled in a more accurate way than it is customary in the Boussinesq approximation. The derivation of the model should make one realize that the purpose of the model has to be kept in mind. We distinguish between the (quantitative) validity of the model, which concerns the quantitative accuracy with which real phenomena are described by the model, and its (qualitative) relevance, which is the usefulness of the model in the study of certain properties or development of new methods that later may be applied in a more complicated situation of the full equations.

Consider a layer of inviscid, incompressible fluid, of infinite extent in one spatial direction (the x-axis); the atmosphere above the layer is assumed to be pressure-free, and the surface tension is neglected. The depth of the layer, to be denoted by H, is the only relevant length scale with which all quantities will be normalized. The full equations describing the layer are well known: the continuity equation in the interior (leading to the Laplace problem for the fluid potential), and the kinematic and Bernoulli's equation at the free surface of the layer. The linear theory for surface waves is well known; infinitesimal surface waves are described by a dispersive wave equation with the dispersion relation given by

$$\omega = \Omega(k) \equiv k\sqrt{\frac{\tanh(k)}{k}}. \tag{1}$$

Here, a scaling of time has been performed such that the (maximal) phase velocity of infinitely long waves is normalized to one, and k and ω denote the scaled wave number and frequency, respectively.

To describe also nonlinear effects in a simplified model, it is common to introduce two parameters: ε for measuring wave amplitudes and μ as a measure of the inverse wavelength. Then, looking for small-amplitude waves, i.e. ε is small, solutions in the form of a series expansion in ε are substituted in the governing equations. Often also the parameter μ is treated as a small quantity, referring to "long waves"; for instance, the well-known Boussinesq approximation, looking for "rather small, rather long waves", is obtained for the relation $\mu = \sqrt{\varepsilon}$. The governing equations, correct up to the second order in ε, are of Boussinesq type and of the second order in time, being a model for bidirectional wave propagation. Restricting once more to waves "mainly" running in one direction then leads to approximated unidirectional wave equations that are of the first order in time. These equations are of KdV type, and, being correct up to the second order, are given by

$$\partial_t u = -\partial_x \left[Ru + \frac{3}{4} u^2 \right], \tag{2}$$

where $u(x,t)$ denotes the (scaled) wave elevation. The quadratic nonlinearity is characteristic of equations of this order of accuracy in ε. The operator R is a (pseudo-) differential operator and accounts for the dispersion properties. For instance, in the Boussinesq approximation, the operator R is a differential operator

$$R_{KdV} = 1 + \partial_x^2 ,$$

and the equation becomes the famous KdV equation.

Let us now review the assumptions of the derivation, taking into account the waves that are most relevant in the laboratory situation. In these cases, waves with a height of not more than 10% of the depth are considered (higher waves are known to break); this corresponds to the wave amplitude of the order $\varepsilon = 0.05$. In the Boussinesq assumption, the corresponding waves would have the wavelength $1/\sqrt{\varepsilon} \approx 5$, i.e. five times the depth. However, in laboratory practice waves with wavelengths between 1 and 3 are dominant. This means that the KdV dispersion given by the operator R_{KdV} is not accurate enough. Indeed, comparison of the KdV dispersion relation, $\omega = k(1-k^2)$, with the exact dispersion for infinitesimal waves given by (1), shows large quantitative and qualitative differences for the relevant wave numbers. This motivates us to use an operator R for which the linearized equation (2) has correct dispersive properties; it means that R is a pseudodifferential operator with the symbol

$$\hat{R}(k) = \sqrt{\frac{\tanh(k)}{k}} . \tag{3}$$

It turns out that this operator performs much better than the KdV dispersion. A characteristic property of this operator is the fact that it is an (nonlocal) integral

operator with a rather large spatial extent. The kernel of this integral operator cannot be expressed in elementary functions (as far as we know); the plot of the kernel (see [3]) shows a rather slow, oscillatory decrease; for instance, the values of $2 \times 10^{-1}, 2 \times 10^{-2}$, and 2×10^{-3} are found at the distances (in units of water depth) of $1, 3.5$, and 10, respectively. This slow decrease implies a long range of interaction between (infinitesimal) surface waves.

At this point it makes sense to give a warning that, as it is customary in such asymptotic methods, the derivation does not provide any information about the validity itself. This means that neither explicit bound for the wave height, nor the spatial or temporal interval for which the solution is accurate can be deduced. This "fact of life" is rather unpleasant, and its *quantitative validity* should be investigated thoroughly. However, the equation does have the essential ingredients of the full surface wave problem – dispersion and nonlinearity. Therefore it can be used to develop new methods and concepts that can later be employed for a more intricate full set of surface wave equations: the model is *qualitatively relevant.*

3. FORMAL SECOND-ORDER SOLUTIONS

In this section we will discuss the properties of the equation by actually "solving" it in a general way whereas a characteristic bichromatic wave is investigated in detail. Knowing that the model equation is derived to be valid in the second order, we will present second-order solutions. The method below provides the formal general solution in this order of accuracy, using Fourier-integral methods and simple series expansions. In general, we will look for the solution of the form

$$u(x,t) = \int \hat{u}(x,\omega) e^{-i\omega t} d\omega \,.$$

The starting-point is the linearized equation, which is a simple dispersive equation with solutions of the form

$$u^{(1)}(x,t) = \int a(\omega) e^{i\{K(\omega)x - \omega t\}} d\omega \,,$$

where K is the inverse of the function Ω

$$\omega = \Omega(k) \Leftrightarrow k = K(\omega),$$

so that $e^{i\{K(\omega)x-\omega t\}}$ are the monochromatic modes with the frequency ω, and $a(\omega)$ is the wave spectrum. Assuming a to be small, of order ε, the solution of (2) correct up to order ε^2 is obtained by iteration:

$$u(x,t) = u^{(1)}(x,t) + u^{(2)}(x,t),$$

where, in the spectral space, the linear and nonlinear terms are given by

$$\hat{u}(x,\omega) = \hat{u}^{(1)}(x,\omega) + \hat{u}^{(2)}(x,\omega)$$
$$= a(\omega)e^{iK(\omega)x} + \int a(s)\Gamma(\omega,s)a(\omega-s)e^{i\{K(s)+K(\omega-s)\}x}ds\,. \quad (4)$$

Here, the expression $\Gamma(\omega,s)$ is a consequence of the nonlinear interaction between the wave with the frequency s and the one with the frequency $(\omega - s)$ that, together, produce the frequency ω; the expression is explicitly given by

$$\Gamma(\omega,s) = \frac{K(s)+K(w-s)}{w-\Omega[K(s)+K(w-s)]}\,.$$

It should be noted that the formula gives the general solution in terms of the spectral function $a(\omega)$. The result implies that the complete wave field, at each position, for each time, can be deduced from a given point measurement, i.e. from the signal $\sigma(t)$ that is the wave height as the function of time at one position. Taking the position to be $x = 0$ for simplicity, $u(x = 0,t) = \sigma(t)$, and with $\hat{\sigma}(\omega)$ the spectrum of the signal, the spectral function a should be found from the integral equation

$$\hat{u}(x=0,\omega) = \hat{\sigma}(\omega) = a(\omega) + \int a(s)\Gamma(\omega,s)a(\omega-s)ds\,.$$

In the second order, the solution is found after two iterations by

$$a(\omega) = \hat{\sigma}(\omega) - \int \hat{\sigma}(s)\Gamma(\omega,s)\hat{\sigma}(\omega-s)ds\,.$$

This then leads to the explicit solution of the wave field given by (4). The method presented here is to some degree a generalization of the methods used in [4,5].

3.1. Monochromatic waves

The simplest solution is the second-order variant of a monochromatic wave. Taking for $a(\omega)$ a point spectrum at ω_1, the solution consists of the monochromatic mode plus a "second harmonic" wave:

$$u(x,t) = a_1\cos(k_1x - \omega_1 t) + b_1\cos 2(k_1x - \omega_1 t),$$

where $k_1 = K(\omega_1)$ and

$$b_1 = \frac{3}{2}a_1^2\frac{k_1}{2\omega_1 - \Omega(2k_1)}\,.$$

The second harmonic is often called the "bound wave", which is motivated by the fact that it is intimately related to the first-order harmonic; it is not a solution of the linearized equation, since the dispersion relation is not satisfied: $\Omega(2k_1) \neq 2\Omega(k_1)$. Furthermore, although its length is only half of that of the first-order wave, the phase velocity is the same.

The effect of the second harmonic shows itself most clearly in the profile: the periodic cosine-profile is deformed such that the valleys become flatter and the crests steeper. This combined effect gives also the impression that the wave profile is shifted upwards, although the spatial average over one period remains zero. The waveform is recognized as the graph of a cnoidal function; for brevity, in the following we will call these nonlinear modes. This qualitative effect of second harmonic modes can be seen in Fig. 2.

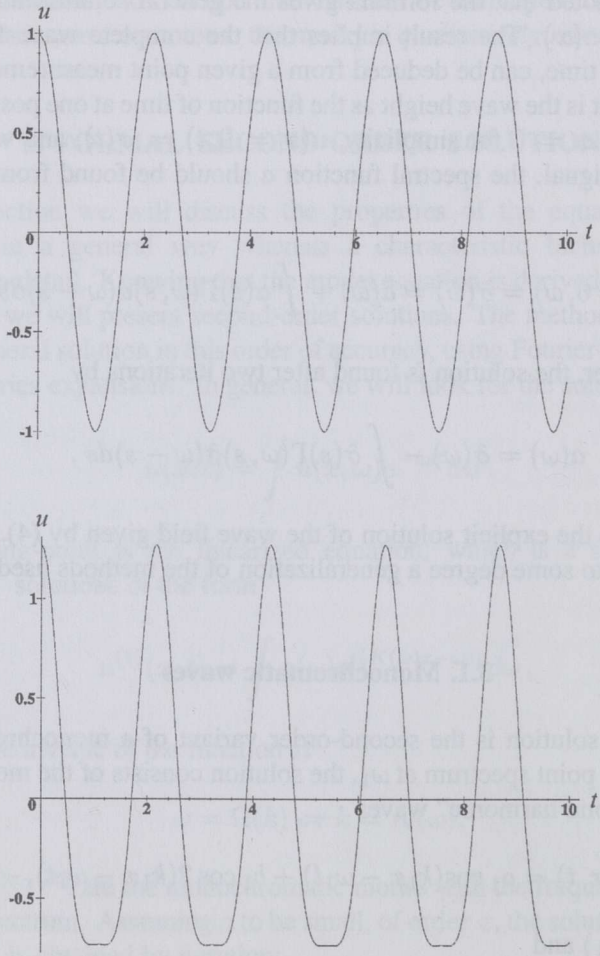

Fig. 2. The qualitative effect of second harmonic modes (below) on monochromatic waves (above).

3.2. Bichromatic waves

A bichromatic wave is the next simplest wave, being composed of the linear superposition of two monochromatic waves with nearly the same frequencies, plus all nonlinear interactions. Neglecting effects of a higher than second order, the nonlinearity produces two bound waves, and a high-frequency and a low-frequency interaction wave:

$$\begin{aligned} u(x,t) = {} & a_1 \cos(k_1 x - \omega_1 t) + a_2 \cos(k_2 x - \omega_2 t) \\ & + b_1 \cos 2(k_1 x - \omega_1 t) + b_2 \cos 2(k_2 x - \omega_2 t) \\ & + \alpha \cos 2(\Delta k x - \Delta\omega t) + \beta \cos 2(\bar{k} x - \bar{\omega} t)\,, \end{aligned} \tag{5}$$

where the wave number and frequency difference have been introduced as small quantities:

$$\bar{k} = \frac{k_1 + k_2}{2}\,,\quad \bar{\omega} = \frac{\omega_1 + \omega_2}{2}\,,\quad \Delta k = \frac{k_1 - k_2}{2}\,,\quad \Delta\omega = \frac{\omega_1 - \omega_2}{2}\,.$$

The dynamic interaction process of these 6 waves, with 3 speeds present, shows complicated spatial patterns and temporal signals. We will investigate this step by step for waves with equal amplitudes $a_1 = a_2 = A$, in which case the other coefficients are given by

$$\begin{aligned} b_m &= \frac{3A^2}{2}\,\frac{k_m}{2\omega_m - \Omega(2k_m)}\,, \\ \alpha &= \frac{3A^2}{4}\,\frac{k_1 - k_2}{\omega_1 - \omega_2 - \Omega(k_1 - k_2)}\,, \\ \beta &= \frac{3A^2}{2}\,\frac{k_1 + k_2}{\omega_1 + \omega_2 - \Omega(k_1 + k_2)}\,. \end{aligned}$$

Linear interference of the first-order waves shows the characteristic picture of beats; the pattern is displayed in Fig. 3.

The envelope is harmonic with a "long" wavelength $2\pi/\Delta k$ which is found from

$$\cos(k_1 x - \omega_1 t) + \cos(k_2 x - \omega_2 t) = 2\cos(\Delta k x - \Delta\omega t)\cos(\bar{k} x - \bar{\omega} t), \tag{6}$$

and this envelope translates with the speed $\frac{\Delta\omega}{\Delta k}$ which is approximately the group velocity at the average wave number. This linear interference pattern is one of the most beautiful phenomena of nature, and it is a remarkable fact that it can be described in such a simple mathematical form given by the formula above. Actually, interference patterns of nonharmonic functions are just as interesting. By way of example we show the linear interference pattern of two nonlinear modes. In that case the coefficients b_1 and b_2 will differ only slightly. The result of the interference pattern is shown qualitatively in Fig. 4 as the time signal.

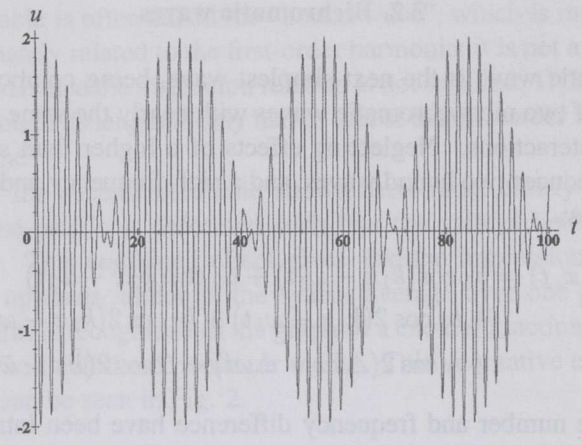

Fig. 3. Linear interference of the first-order bichromatic waves (beats).

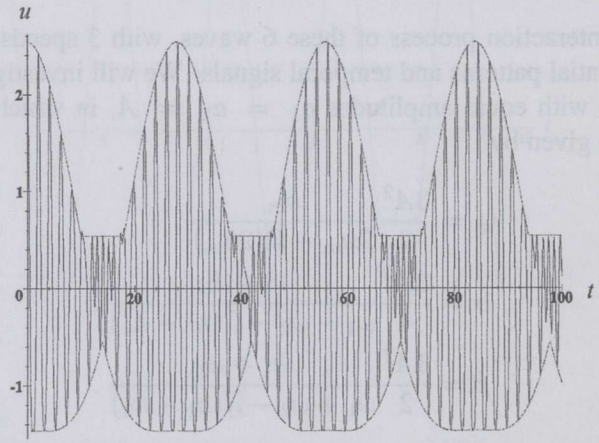

Fig. 4. Qualitative interference pattern of nonharmonic modes on the first-order bichromatic waves (beats) and the envelope.

The envelope has a part of (almost) horizontal lines at intervals where the waves are out of phase, as is well seen in Fig. 5. In these regions, the (upper) envelope is shown by a straight line at the height $(A + b) - (A - b) = 2b$. This picture clearly reveals the complicated details. Taken together, the envelope is given by

$$\begin{aligned}\text{envelope} \;=\; \max / \min\{&2b, 2A\cos(\Delta kx - \Delta\omega t) + 2b\cos 2(\Delta kx - \Delta\omega t),\\ &-2A\cos(\Delta kx - \Delta\omega t) + 2b\cos 2(\Delta kx - \Delta\omega t)\}\,.\end{aligned}$$

Except for the flat parts of the upper envelope, the characteristic form of the nonlinear mode is clearly present in the envelope and its formula. Observe that, just as for linear modes, the propagation speed is approximately the group velocity.

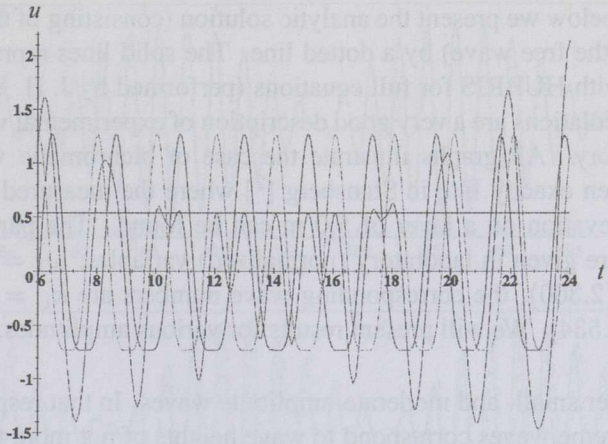

Fig. 5. Components of the envelope of bichromatic waves in Fig. 4.

3.3. Free waves generated in experiments

In order to make a precise comparison of analytic solutions with experimental data, one additional effect from the actual generation of the waves should be taken into account, the effect of so-called *free waves*. For practical reasons, the steering of the wave generator consists of harmonic motions, leading to harmonic signals. Whatever the generated realized wave field will be, it should be compatible at the wavemaker with the given motion. This implies that our analytic solutions should be compensated in such a way that at the wavemaker their time signal equals the signal of the wave generator motion. This will be done in the following, assuming that the effect of the wave generator can be translated in a given harmonic signal at the position $x = 0$, for instance, for a bichromatic wave in a time signal with two frequencies:

$$generator(t) = a_1 \cos(\omega_1 t) + a_2 \cos(\omega_2 t)\,. \tag{7}$$

For the wave field to be compatible with the generator, we require $generator(t) = u(x = 0, t)$, which can be achieved by adding harmonic waves of opposite sign with the same frequency as the second-order harmonics that are present in the second-order theory. This modification is done below when we compare experimental/numerical data with analytic solutions.

3.4. Comparison of experimental and analytic results

In this subsection we show that for small-amplitude waves, the analytic solutions given above describe quite well the actual waves as shown in Figs. 6–8.

In the graphs below we present the analytic solution (consisting of the second-order solution with the free wave) by a dotted line. The solid lines represent numerical calculations with HUBRIS for full equations (performed by J. H. Westhuis); these numerical calculations are a very good description of experimental waves generated in the laboratory. All graphs illustrate the case of bichromatic waves; the data have been taken exactly like in Stansberg [2] where the measured time signals of the surface elevation on a layer of 5.0 m can be found. The parameters for the biharmonics are given in laboratory (normalized) variables: $\omega_1 = 2.992\ (2.136)$, $\omega_2 = 3.222\ (2.300)$; the corresponding wave numbers are $k_1 = 1.070\ (5.349)$, $k_2 = 0.907\ (4.534)$. We will present results for various amplitudes, but in all cases $a_1 = a_2 \equiv a$.

We consider small- and moderate-amplitude waves. In that respect it should be noted that extreme waves correspond to wave heights of not more than 10% of the

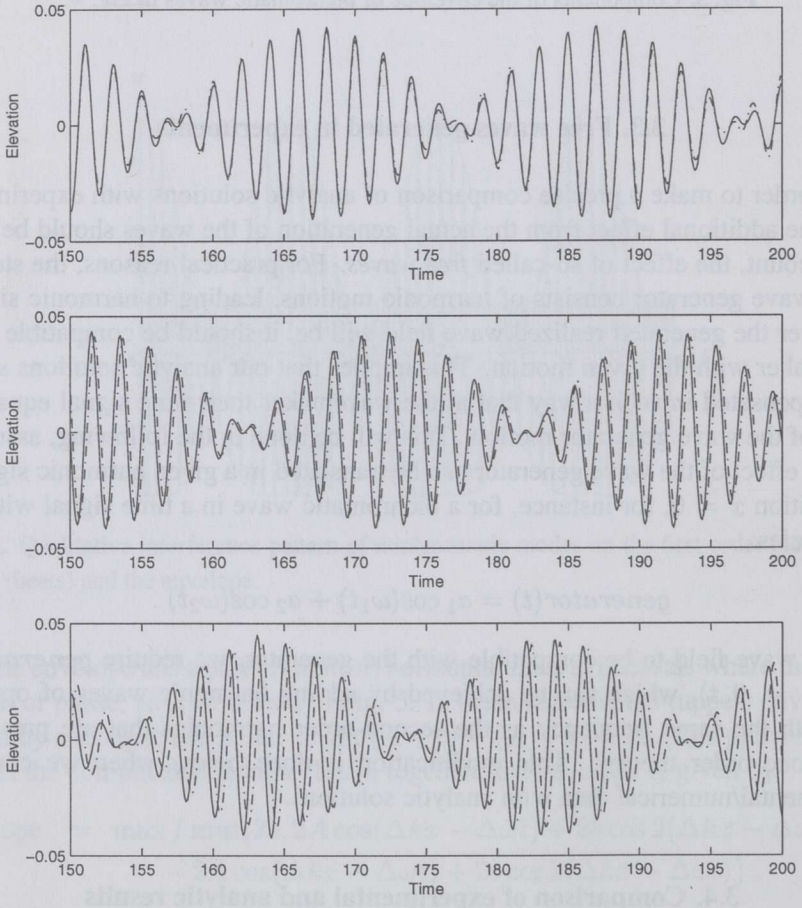

Fig. 6. Small-amplitude waves at X = 10, 80, 160, computed using HUBRIS (solid line) and according to the second-order theory (dashed line).

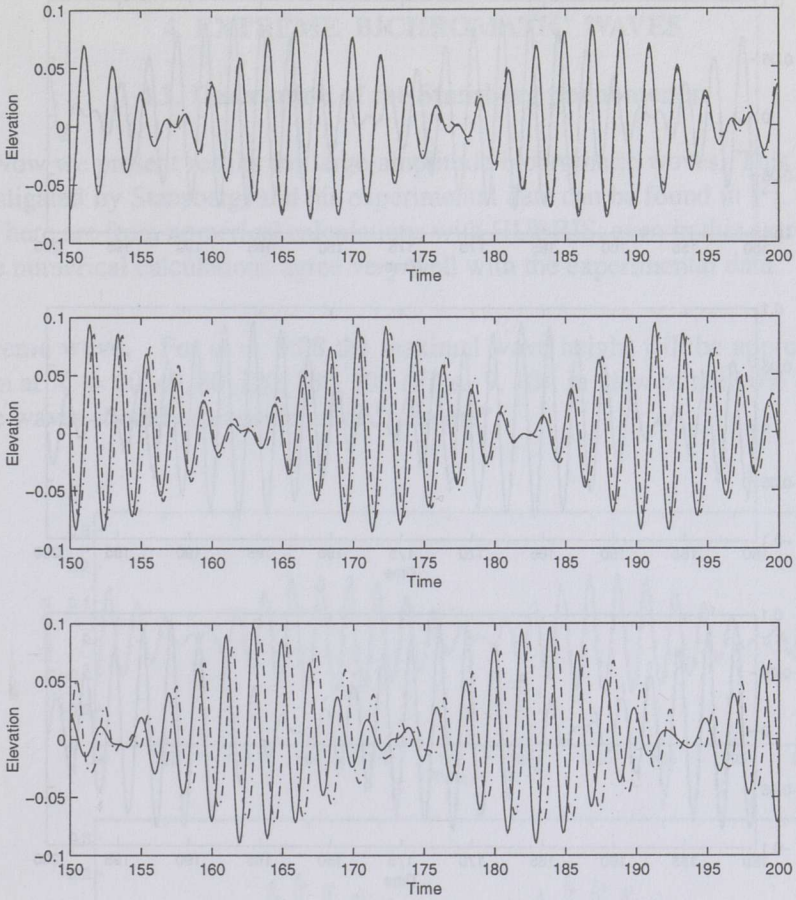

Fig. 7. Same as Fig. 6 for moderate waves.

depth, i.e. 0.50 m in laboratory variables. In Figs. 6–8 are given time signals at different positions. We use X to denote the position in laboratory variables, related to the scaled variables x given by $X = xH$, where $H = 5$ is the depth of the basin. The actual wave is generated (in the laboratory) at $X = 0$; the measured/calculated signal at $X = 10$ is taken to calibrate the phases of the analytic bichromatic (using the least-squares method). It should be noted that in these 10 m the nonlinearity has already produced some effect, since the matching shows little deviation.

Small-amplitude wave. For the amplitude $a = 0.02$ the maximal wave height will be approximately 0.08 m at $X = 10, 80, 160$ (Fig. 6).

Moderate-amplitude wave. For the amplitude $a = 0.04$ the maximal wave height will be approximately 0.20 m at $X = 10, 80, 160$ (Fig. 7).

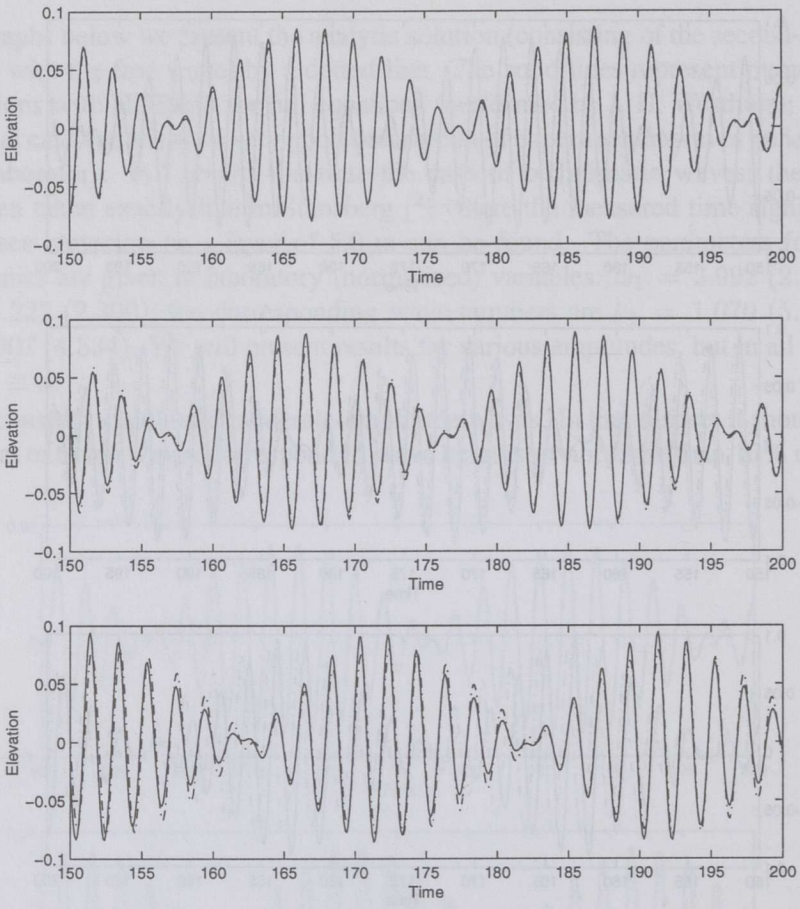

Fig. 8. Moderate-amplitude waves at $X = 10, 40, 80$, computed using HUBRIS (solid line) and according to the second-order theory with phase correction (dashed line).

Discussion. It is clear from these plots that the second-order solution describes the real waves quite well. Taking into account the initial deviations, the most striking difference is an error in the phase velocity: the carrier wave in the second-order theory translates too slowly. An increase in the phase velocity is a typical (higher-order, but well noticeable) nonlinear effect, as we shall see in the next section; adjusting the phase velocity to take this nonlinear effect into account leads to much better results. This is exemplified in Fig. 8 for $a = 0.04$ at $X = 10, 40, 80$, where the phase velocity is increased by the amount (see the next section) of $-\beta(\Delta k)^2/\bar{k}$ which is proportional to a^2.

4. EXTREME BICHROMATIC WAVES

4.1. Description of the Stansberg phenomenon

Now we present results for large-amplitude bichromatic waves. This case was investigated by Stansberg, and his experimental data can be found in [2]. The data used here are from numerical calculations with HUBRIS; even in this extreme case these numerical calculations agree very well with the experimental data.

Extreme wave. For $a = 0.08$ the maximal wave height will be approximately 0.5 m at $X = 10, 40, 80, 120, 160, 200$ (Figs. 9, 10); in view of the 10% criterion, these waves should be considered as "extreme".

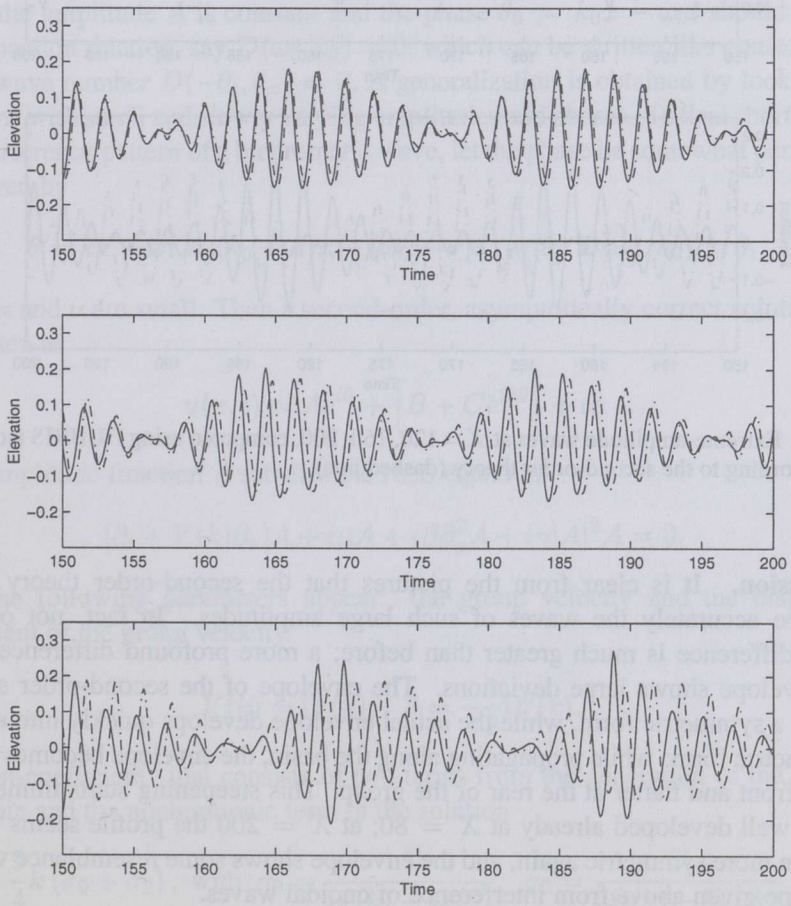

Fig. 9. Extreme-amplitude waves at $X = 10, 40, 80$, computed using HUBRIS (solid line) and according to the second-order theory (dashed line).

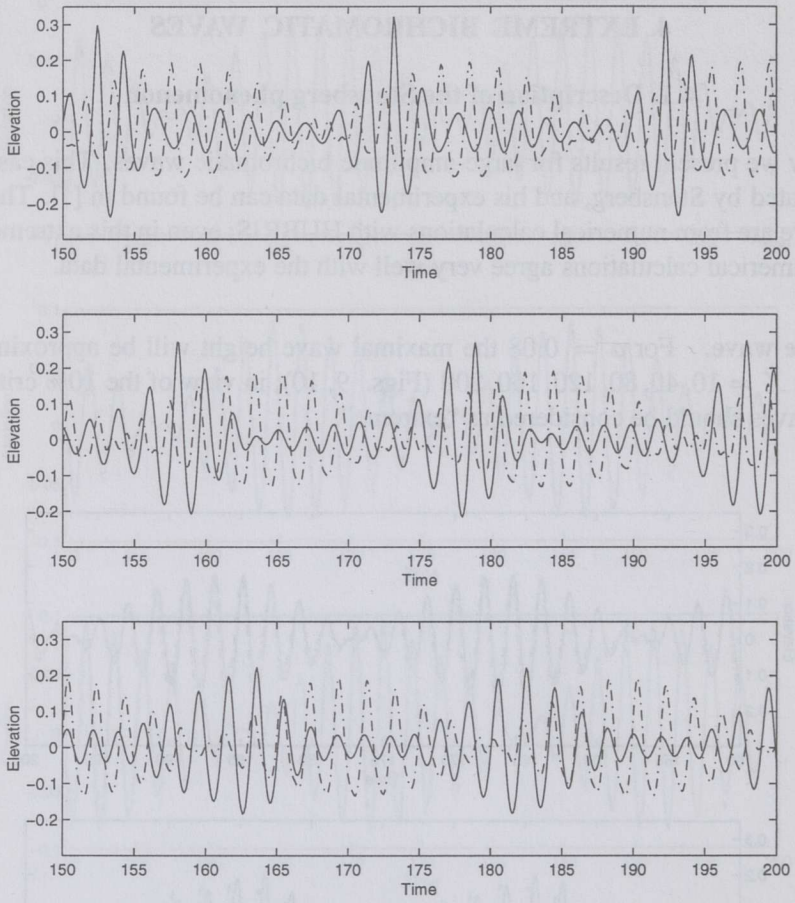

Fig. 10. Extreme-amplitude waves at $X = 120, 160, 200$, computed using HUBRIS (solid line) and according to the second-order theory (dashed line).

Discussion. It is clear from the pictures that the second-order theory cannot describe accurately the waves of such large amplitudes. In fact, not only the phase difference is much greater than before; a more profound difference is that the envelope shows large deviations. The envelope of the second-order solution retains a symmetric form, while the actual envelope develops quickly into a strong asymmetric form: while propagating along the basin, the envelope becomes steeper in the front and flatter at the rear of the group. This steepening starts immediately and is well developed already at $X = 80$; at $X = 200$ the profile seems to have become more symmetric again, and the envelope shows some resemblance with the envelope given above from interference of cnoidal waves.

This phenomenon seems not easy to explain. Stansberg gives a partial description of the evolution of the envelope, using the variations in time of the instantaneous frequencies that he found in the measurements. The basic ingredient

in his (partial) explanation is based on changes in group and phase velocities within one wave group, which can be explained from the "nonlinear" dispersion relation.

4.2. Asymptotic solutions based on NLS

In this subsection we present an alternative way to describe the biharmonic evolution that is capable of explaining the Stansberg effect. The improvement to the second-order solutions described in Section 3 is in the fact that now we look for an asymptotic approximation, based on the phase-amplitude equation. First, we present a brief description of the approximate theory. The starting-point is the fact that monochromatic solutions are of the form

$$u(x,t) = Ae^{i\theta_0} + cc,$$

where the amplitude A is constant and the phase $\theta_0 = k_0 x - \omega_0 t$ should satisfy the dispersion relation, say $D(\omega_0, k_0) = 0$, which can be written like conservation of the wave number $D(-\theta_t, \theta_x) = 0$. A generalization is obtained by looking for solutions with small and slowly varying amplitudes and phases. To deal shortly with the interference pattern of a bichromatic wave, let the phase be somewhat perturbed, say, given by

$$\theta = kx - \omega t \equiv (k_0 + \kappa)x - (\omega_0 + \nu)t, \text{ with } D(\omega_0, k_0) = 0,$$

where κ and ν are small. Then a second-order, asymptotically correct solution can be written as

$$u(x,t) = Ae^{i\theta} + \left[B + Ce^{2i\theta}\right] + cc \tag{8}$$

if the amplitude function A satisfies the NLS equation

$$[\partial_t + V(k)\partial_x]A + i\mu A + i\beta\partial_x^2 A + i\gamma|A|^2 A = 0. \tag{9}$$

Here the following parameters appear: the group velocity and the dispersion coefficient of the group velocity

$$V(k) = \Omega'(k), \quad \beta = -\frac{1}{2}\Omega''(k),$$

the "gen-coefficient" that consists of two terms from the generation of the second harmonic and the nonharmonic term in the solution

$$\gamma = \frac{9}{4}k\left(\sigma_0 + \sigma_2\right), \text{ with } \sigma_0 = \frac{1}{\Omega'(k) - \Omega'(0)}, \quad \sigma_2 = \frac{k}{2\Omega(k) - \Omega(2k)}.$$

The dispersion coefficient of the group velocity β is positive and the gen-coefficient σ_0 is negative, while for wave numbers of interest in the laboratory, the

coefficients σ_2 and γ are positive. At this point the use of a model equation with improved dispersive properties is essential; for instance, for the usual KdV equation, the coefficient γ is negative, and none of the following explanations and properties would be found (see van Groesen [6]). In the asymptotic solution, the amplitudes of the generated waves are expressed in terms of A by

$$B = \frac{3}{4}\sigma_0|A|^2, \quad C = \frac{3}{2}\sigma_2 A^2.$$

Finally, the coefficient μ accounts for the fact that in general the perturbed frequency and wave number do not satisfy the dispersion relation in the third order; it is the *phase mismatch*

$$\begin{aligned} \mu = -\nu + V(k)\kappa &\approx -(\omega - \omega_0) + V(k_0)\kappa - 2\beta\kappa^2 + \mathcal{O}(\kappa^3) \\ &= \Omega(k_0 + \kappa) - \omega + \mathcal{O}(\kappa^3). \end{aligned}$$

In fact, in the special case $\kappa = \nu = 0$, the NLS equation reduces to

$$(\partial_t + V_0\partial_x)A + i\beta_0\partial_x^2 A + i\gamma_0|A|^2 A = 0\,.$$

It is common to introduce a frame moving with the group velocity

$$\xi = x - V_0 t, \quad \tau = t$$

so that the equation becomes

$$\partial_\tau A + i\mu A + i\beta_0\partial_\xi^2 A + i\gamma_0|A|^2 A = 0. \tag{10}$$

The solution given above is an "asymptotic" solution in the sense that now third-order contributions in the solution (that are neglected) will be uniformly bounded; the fact that A should satisfy the NLS equation guarantees that secular terms in the third order vanish, a property that was not satisfied by the "formal" second-order solution considered in the previous section. It follows that this presentation of the solution is much more accurate. However, the drawback is that now another nonlinear equation has to be solved, i.e. the NLS equation. Compared to the original KdV-type equation, the advantage is that the NLS equation can be investigated keeping closely to the physical quantities that seem to dominate the dynamics.

4.3. Bichromatic wave as NLS solution in the lowest order

To study the NLS equation, and to be able to relate it to the partial analysis by Stansberg, let us first see how the bichromatic wave can be obtained in the lowest order. To that end, write the linear bichromatic wave as a modulation of a carrier

wave in the form (6). Clearly, the averaged wave number and frequency will not in general satisfy the dispersion relation. Taking $k_0 = \bar{k}$, observe that

$$\bar{\omega} - \omega_0 \equiv \nu = -\beta_0 (\Delta k)^2 .$$

Then, in the lowest order, for the NLS solution with the phase function as the carrier wave,

$$u = Ae^{i(\bar{k}x - \bar{\omega}t)} + cc,$$

the amplitude should satisfy the NLS equation with the phase mismatch $\mu = -\nu$

$$\partial_\tau A + i\beta_0 (\Delta k)^2 A + i\beta_0 \partial_\xi^2 A + i\gamma_0 |A|^2 A = 0.$$

In the lowest order this gives the solution

$$A = a \cos[\Delta k(x - V_0 t)]$$

which is the modulation term $\cos[(\Delta k)x - (\Delta\omega)t]$ of the bichromatic wave in the required order, since $\Delta\omega = V_0 \Delta k + \mathcal{O}(\Delta k)^3$.

4.4. Phase-amplitude equations for NLS

We will now rewrite the NLS equation (10) for the complex amplitude A with a real amplitude function f and a phase function ϕ as

$$A = \sqrt{E} e^{i\phi} = f e^{i\phi} .$$

Observe that f is the real amplitude, and its square E is (twice) the "energy". With this notation, the actual solution is given by

$$u(x,t) = 2f \cos(\theta + \phi) + 2f^2 \left[B + C \cos(2(\theta + \phi))\right] . \qquad (11)$$

Introducing the variation of the wave number and frequency

$$\kappa = \partial_x \phi, \quad \nu = -\partial_t \phi,$$

so that conservation of the wave number, the kinematic identity $\partial_t \kappa + \partial_x \nu = 0$, is satisfied identically, the equations can be rewritten in various forms. We will use the notation $V = V(k_0 + \kappa) \approx V_0 - 2\beta\kappa$ for the group velocity, and D_t for the material time derivative moving with the group velocity. With this notation, the amplitude/energy equation is found to be

$$(\partial_t + V_0 \partial_x) E = \partial_x \left[2\beta (\partial_x \phi) E\right]$$

which can be written like $\partial_t E + \partial_x(VE) = 0$ or

$$D_t E + E\partial_x V = 0; \tag{12}$$

this is precisely the energy equation used by Stansberg (see below).

The phase equation is a bit more involved; a direct formulation for the phase is

$$[(\partial_t + V_0\partial_x)\phi - \beta(\partial_x\phi)^2]f + \beta\partial_x^2 f + \gamma f^3 = 0 \tag{13}$$

which can be written like

$$\left[-\nu + V_0\kappa - \beta\kappa^2 + \gamma E\right] f + \beta\partial_x^2 f = 0\,.$$

Observe that this is a generalization of the result above where κ and ν were constant. The appearance of the specific combination $V_0\kappa - \beta\kappa^2 + \gamma E$ in the phase equation leads to introduction of the nonlinear dispersion relation

$$\Omega_{nonlin}(k) = \Omega(k) + \gamma E$$

so that $\Omega_{nonlin}(k_0 + \kappa) = \Omega(k_0) + V_0\kappa - \beta\kappa^2 + \gamma E$ and hence

$$-\nu + V_0\kappa - \beta\kappa^2 + \gamma E = \Omega_{nonlin}(k_0 + \kappa) - \omega$$

is recognized as the phase mismatch in this case.

The phase velocity is affected like

$$V_{nonlin}^{phase}(k) = V_{lin}^{phase}(k) + \gamma\frac{E}{k},$$

which is a simple explanation of the phase lag that was observed above in the plots for small-amplitude waves. This modification of the phase velocity has been taken to improve the second-order results above by approximating the energy by some averaged value.

Finally we shall observe alternative ways to describe the phase equation. Differentiating with respect to x gives

$$\partial_t\kappa + \partial_x\left[V_0\kappa - \beta\kappa^2\right] = -\partial_x\left[\frac{\beta\partial_x^2 f}{f} + \gamma E\right]$$

which can also be written as an evolution equation for the group velocity:

$$\partial_t V + V\partial_x V = 2\beta\partial_x\left[\frac{\beta\partial_x^2 f}{f} + \gamma E\right]. \tag{14}$$

4.5. Explanation of the phenomenon

Stansberg gives a semiempirical explanation of the phenomenon along the following lines. He solves the energy equation $D_t E = -E\partial_x V$ by updating the amplitude E with the Euler forward method. However, he does not use (as he mentions explicitly) the kinematic wave equation, i.e. the phase equation above. Instead, he estimates the change $\partial_x V$ by using the approximation for the kinematic equation

$$\partial_t V \approx -V\partial_x V, \tag{15}$$

where he exploits this equation in an ingenious way by applying on the right-hand side an estimate for the group velocity by extracting from the experiment the instantaneous frequency at each position of measurement.

Equation (15) is actually an approximation of (14). Together with the energy equation these equations form a closed system of nonlinear equations (note $E = f^2$). Observe that neglecting the term $\frac{\beta\partial_x^2 f}{f}$ (that introduces dispersion in the equations) it would be a set of first-order (nonhyperbolic) equations, showing the phenomenon of breaking. We will not investigate here the equations in this generality; instead, we shall explain the phenomenon in the following approximative way.

At the initial position where the wave is generated, we can assume the wave to be nearly linear bichromatic, which was shown in Subsection 4.3 to be described by taking

$$\nu = -\beta(\Delta k)^2, \quad f = a\cos[(\Delta k)(x - V_0 t)]\,.$$

From the phase equation $\left[-\nu + V_0\kappa - \beta\kappa^2 + \gamma E\right] f + \beta\partial_x^2 f = 0$, the first term suggests the approximation

$$V_0\kappa - \beta\kappa^2 + \gamma E = 0.$$

We solve this equation approximately for κ as $\kappa = -\frac{\gamma E}{V_0}$, which then leads to an approximation for the group velocity

$$V = V_0 - 2\beta\kappa = V_0 + \frac{2\beta\gamma}{V_0}E.$$

The last expression shows that the group velocity depends in a specified way on the energy: the larger the amplitude, the larger the group velocity. Adjusting the amplitude function to the changing group velocity leads to the updated amplitude:

$$f = a\cos\left[(\Delta k)(x - Vt)\right], \text{ with } V = V_0 + \frac{2\beta\gamma}{V_0}a^2\cos^2[(\Delta k)(x - V_0 t)].$$

The phase function is given approximately by

$$\phi = \beta(\Delta k)^2 t - \frac{\gamma E}{V_0} x \text{ with } E = a^2 \cos^2[(\Delta k)(x - V_0 t)].$$

In this way the evolution of the envelope can be followed along the basin in an iterative way. The solution given here is only approximate, stressing the evolution from the linear limit to the bichromatic limit. Nevertheless, numerical results show the tendency of Stansberg's phenomenon. Some numerical results are shown in Fig. 11, recorded at $x = 0, 16, 32$ in the normalized value. Taking the wave basin depth to be 5.0 m, the corresponding physical positions are at $X = 0, 80, 160$.

5. CONCLUSION AND DISCUSSION

In this paper we presented a KdV-type equation to model the behaviour of surface waves as they appear in experiments performed in hydrodynamic laboratories. A critical investigation of the relevant waves showed the necessity to use a model that describes the dispersive properties of waves with rather small lengths; this led us to consider the dispersion as known for linear theory, thereby introducing an integral rather than a differential operator. The practical problems associated with such a nonlocal operator were solved, while the use of this improved dispersion was critical to achieve a reliable description and explanation of the phenomena.

A second-order theory that formally gives the general solution of the equation was shown to perform quite well for waves with small or moderate amplitudes. The main discrepancy is an error in the phase velocity, which was observed by comparing experimental results with very accurate numerical solutions of bichromatic waves. This phase error could be reduced by using the phase velocity as predicted by the nonlinear dispersion relation. It should be noted that since this error can be attributed to the approximate nature of the analytical *solution*, the good agreement confirms the validity of the *model equation* as a simplified description of the surface wave problem.

The relevance of the model equation was strongly supported by its successful use in case of extreme bichromatic waves. In order to explain the phenomenon observed and described by Stansberg, the approximate solution technique had to be adjusted to deal with the waves of extremely large amplitudes. Adding to the semiempirical explanation given by Stansberg, we derived a complete set of phase-amplitude equations that should describe the phenomenon of large deviations of the envelope of bichromatic waves. Approximate analytical and numerical investigations of these equations showed that the observed phenomenon can be described and explained, at least qualitatively. In a subsequent paper we will deal with this problem in more detail.

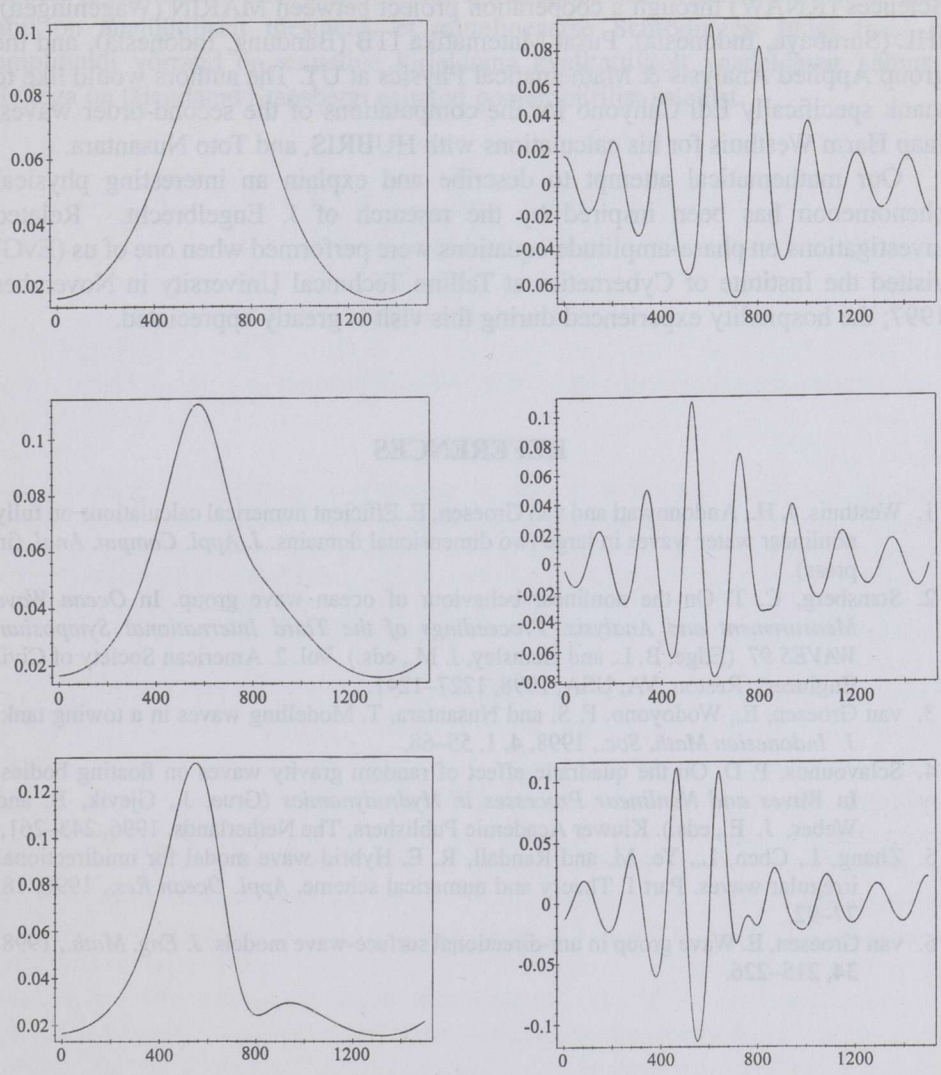

Fig. 11. Numerical simulation of extreme-amplitude bichromatic waves (right, second-order effects are added) and their envelopes f recorded at $x = 0, 16, 32$ in normalized variables. The horizontal axis shows the number of time discretization while the vertical axis shows the normalized elevation.

ACKNOWLEDGEMENTS

This work is part of the Scientific Cooperation between The Netherlands and Indonesia, financially supported by the Royal Netherlands Academy of Arts and Sciences (KNAW) through a cooperation project between MARIN (Wageningen), IHL (Surabaya, Indonesia), Pusat Matematika ITB (Bandung, Indonesia), and the group Applied Analysis & Mathematical Physics at UT. The authors would like to thank specifically Edi Cahyono for the computations of the second-order waves, Jaap Harm Westhuis for his calculations with HUBRIS, and Toto Nusantara.

Our mathematical attempt to describe and explain an interesting physical phenomenon has been inspired by the research of J. Engelbrecht. Related investigations on phase-amplitude equations were performed when one of us (EvG) visited the Institute of Cybernetics at Tallinn Technical University in November 1997; the hospitality experienced during this visit is greatly appreciated.

REFERENCES

1. Westhuis, J. H., Andonowati and van Groesen, E. Efficient numerical calculations on fully nonlinear water waves in large two dimensional domains. *J. Appl. Comput. Anal.* (in press).
2. Stansberg, C. T. On the nonlinear behaviour of ocean wave group. In *Ocean Wave Measurement and Analysis. Proceedings of the Third International Symposium WAVES 97* (Edge, B. L. and Hemsley, J. M., eds.). Vol. 2. American Society of Civil Engineers, Reston, VA, USA, 1998, 1227–1241.
3. van Groesen, E., Wodoyono, F. S. and Nusantara, T. Modelling waves in a towing tank. *J. Indonesian Math. Soc.*, 1998, **4**, 1, 55–68.
4. Sclavounos, P. D. On the quadratic effect of random gravity waves on floating bodies. In *Waves and Nonlinear Processes in Hydrodynamics* (Grue, J., Gjevik, B. and Weber, J. E., eds.). Kluwer Academic Publishers, The Netherlands, 1996, 243–261.
5. Zhang, J., Chen, L., Ye, M. and Randall, R. E. Hybrid wave model for unidirectional irregular waves. Part I. Theory and numerical scheme. *Appl. Ocean Res.*, 1996, 18, 77–92.
6. van Groesen, E. Wave group in uni-directional surface-wave models. *J. Eng. Math.*, 1998, **34**, 215–226.

BIKROMAATILISTE PINNALAINETE MITTELINEAARSED NÄHTUSED

E. van GROESEN, ANDONOWATI ja E. SOEWONO

Vaadeldud on Stansbergi laboratoorses eksperimendis kirjeldatud suure amplituudiga bikromaatiliste pinnalainete nähtust. Kasutades Kortewegi–de Vriesi tüüpi

võrrandis täpsemat dispersiooni kirjeldust, mis on vajalik eksperimendis esinevate suhteliselt lühikeste lainepikkuste tõttu, on näidatud, et selle teist järku arendus kirjeldab üsnagi hästi väikese ja mõõduka amplituudiga laineid. Suure amplituudiga lainete korral osutub teist järku teooria aga ebapiisavaks. Asümptootilise mudeli abil on analüütiliselt tõestatud, et mittelineaarse Schrödingeri tüüpi faasi ja amplituudi võrrand on suuteline kirjeldama kvalitatiivselt vaadeldavat nähtust. Sellega on täiendatud Stansbergi esitatud poolempiirilist seletust.